Electronic Supplementary Information

In-situ formed N-containing copper nanoparticles: a high-performance catalyst toward carbon monoxide electroreduction to multicarbon products with high Faradaic efficiency and current density

Huitong Du,[a] Li-Xia Liu,[a] Yanming Cai,[a] Ying Wang,[b] Jian-Rong Zhang,[a] Qianhao Min,[a] and Wenlei Zhu,[a]*

[a]School of Chemistry and Chemical Engineering, School of the Environment, State Key Laboratory of Analytical Chemistry for Life Science, Nanjing University, Nanjing, 210023, P. R. China

[b]College of Environmental Science and Engineering, Tongji University, Shanghai 200092, P. R. China

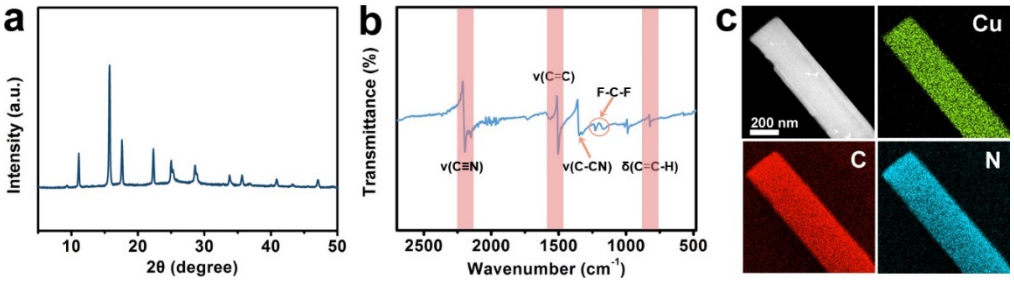

Fig. S1. (a) XRD pattern, (b) FTIR spectrum, (c) TEM image and elemental mapping images of the CuTCNQ.

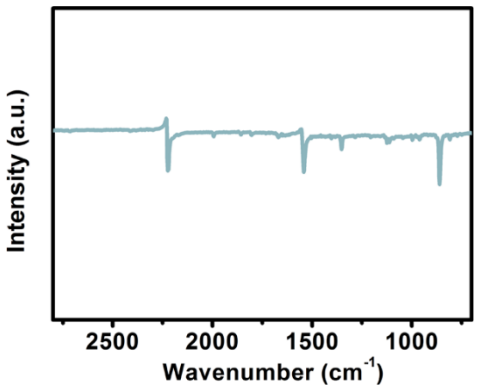

Fig. S2. FTIR spectrum of the TCNQ.

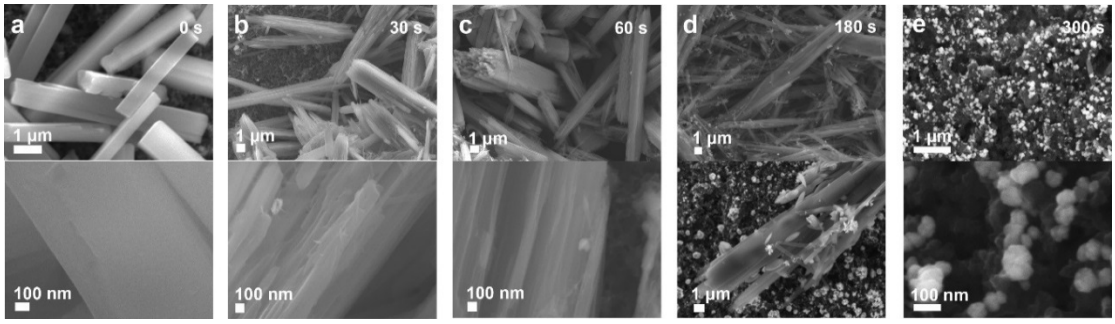

Fig. S3. SEM images of CuTCNQ/GDL at different pre-reduction times under a constant current density of 50 mA cm^{-2}.

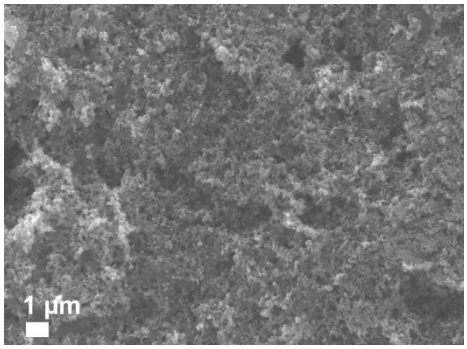

Fig. S4. SEM image of the bare GDL.

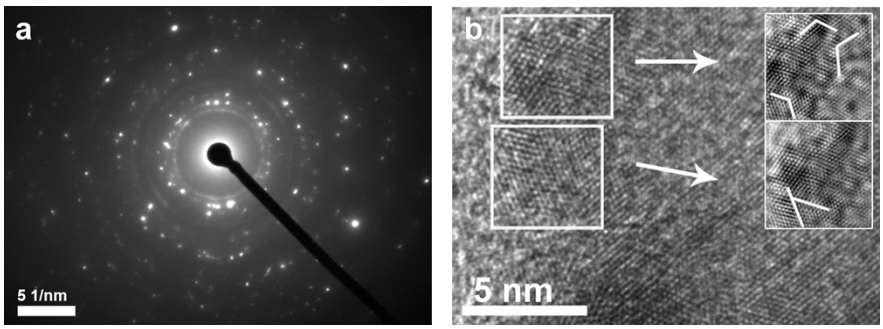

Fig. S5. (a) Selected area electron diffraction (SAED) pattern image of the reconstructed N-Cu NPs. (b) HRTEM images of the N-Cu NPs (Insets present the the grain boundary).

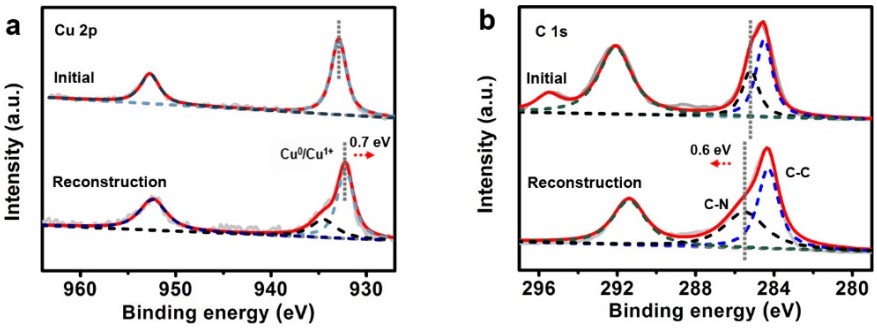

Fig. S6. XPS spectrum in the (a) Cu 2p and (b) C1s regions for N-Cu NPs and CuTCNQ.

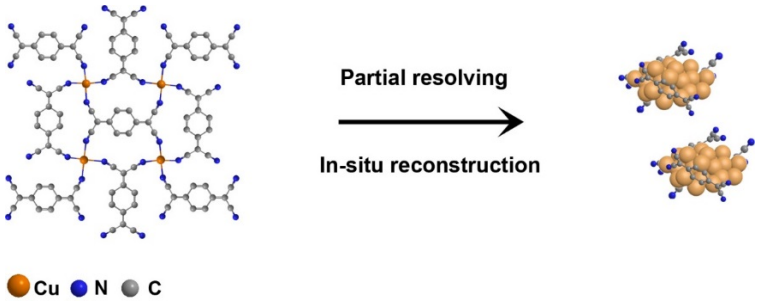

Fig. S7. Schematic diagram of the proposed N-Cu NPs evolution.

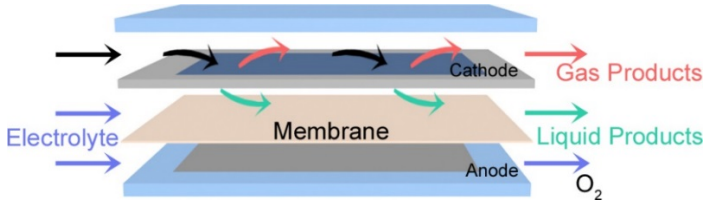

Fig. S8. Schematic diagram of the flow cell.

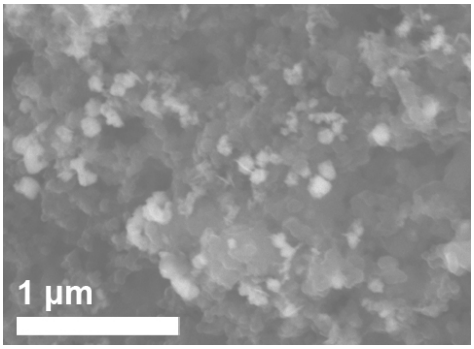

Fig. S9. SEM image of N-Cu NPs/GDL after durability test.

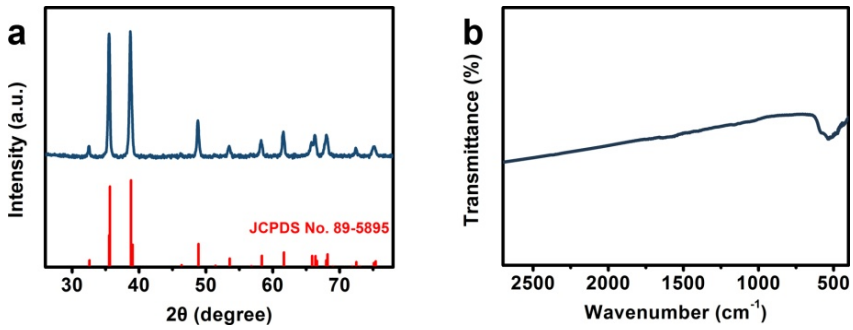

Fig. S10. (a) XRD pattern and (b) FTIR spectrum of CuO NPs.

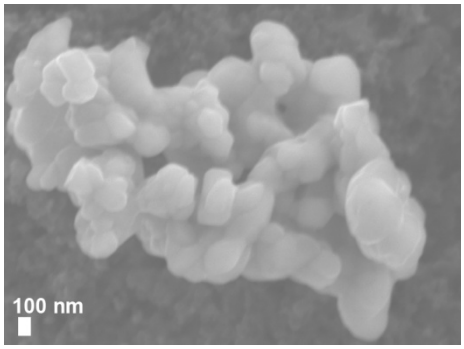

Fig. S11. SEM image of CuO NPs/GDL.

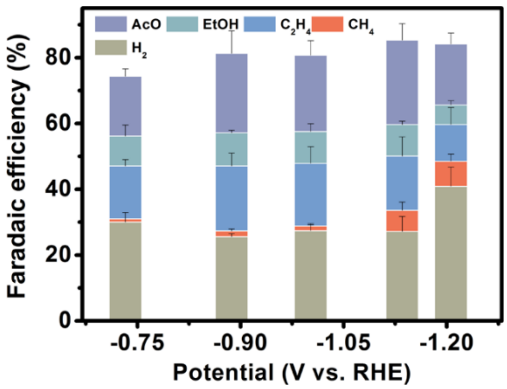

Fig. S12. ECOR products distribution of CuO NPs/GDL at each given potential in 1.0 M KOH.

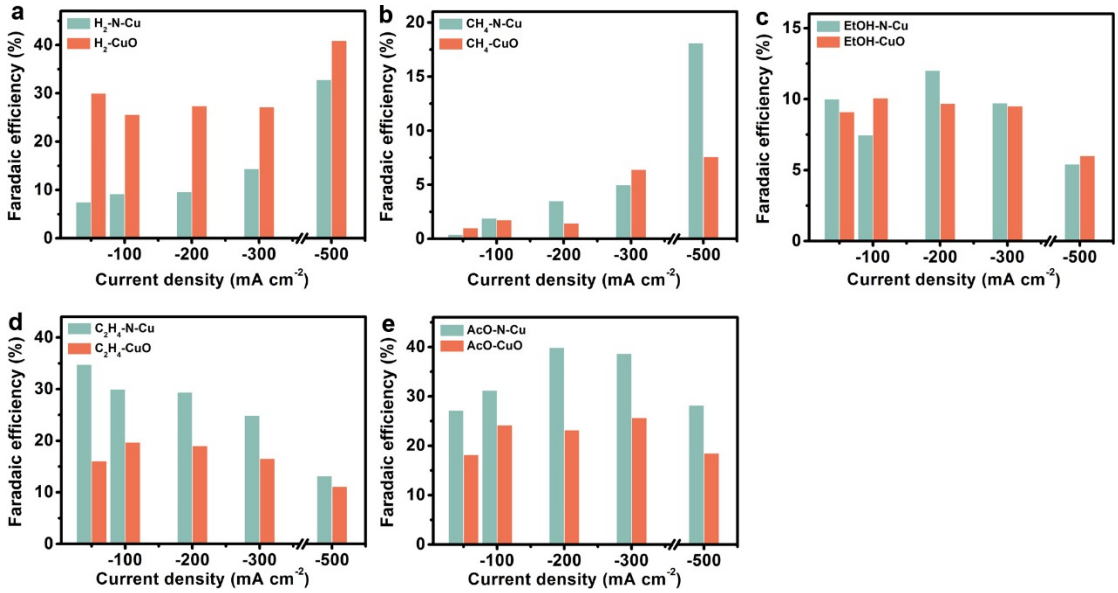

Fig. S13. (a) H_2, (b) CH_4, (c) EtOH, (d) C_2H_4 and (e) AcO FEs of N-Cu NPs/GDL and CuO NPs/GDL at each given current density in 1.0 M KOH.

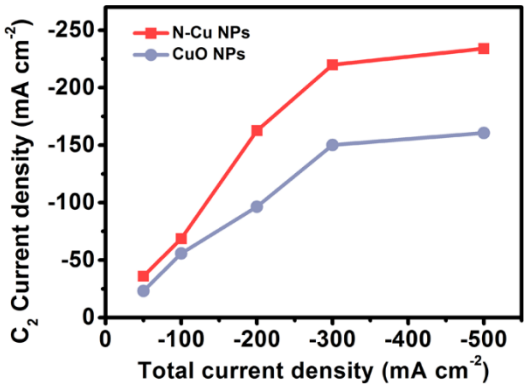

Fig. S14. C_2 partial current density for N-Cu NPs/GDL and CuO NPs/GDL at each given total current density in 1.0 M KOH.

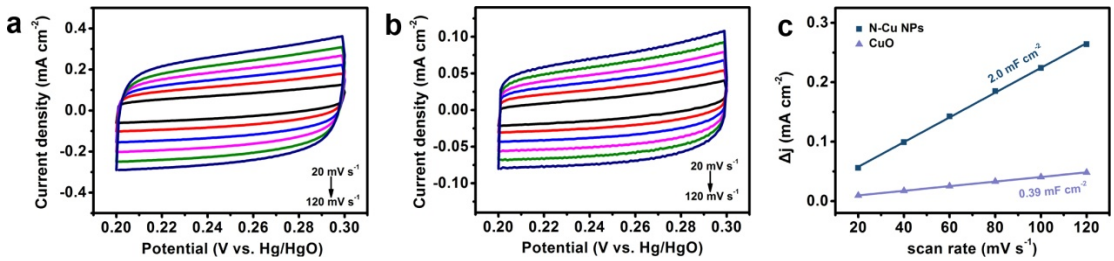

Fig. S15. CVs of (a) N-Cu NPs/GDL and (b) CuO NPs/GDL with various scan rates in the range between 0.2 V and 0.3 V, (c) The capacitive currents at 0.25 V as a function of scan rate for N-Cu NPs/GDL and CuO NPs/GDL.

According to the above formula, the calculated ECSA of N-Cu NPs/GDL and CuO NPs/GDL are 68.97 and 13.45 cm^2_{ECSA}, respectively. Additionally, we can determine the RFs of N-Cu NPs/GDL and CuO NPs/GDL are 68.97 and 13.45, respectively.

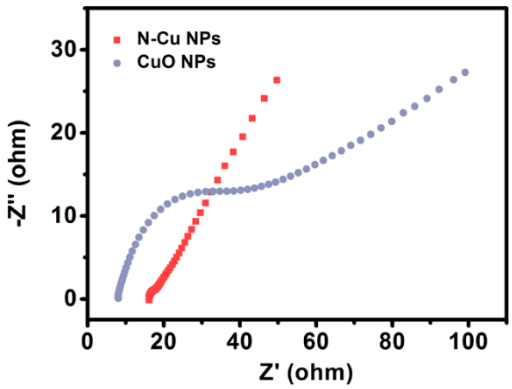

Fig. S16. Nyquist plots of N-Cu NPs/GDL and CuO NPs/GDL.

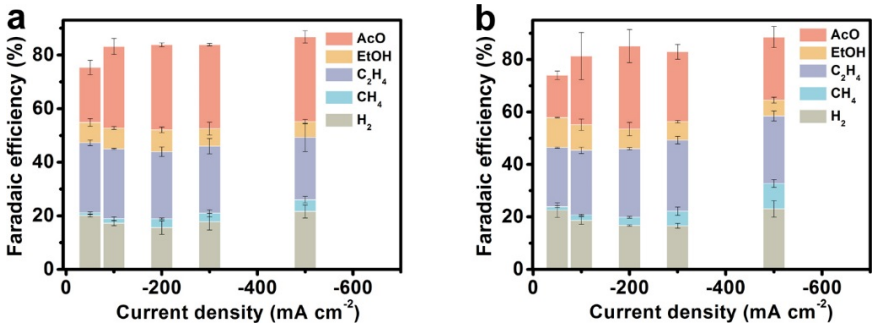

Fig. S17. ECOR products distribution of (a) Cu NPs/GDL and (b) CuCl/GDL at each given current density in 1.0 M KOH.

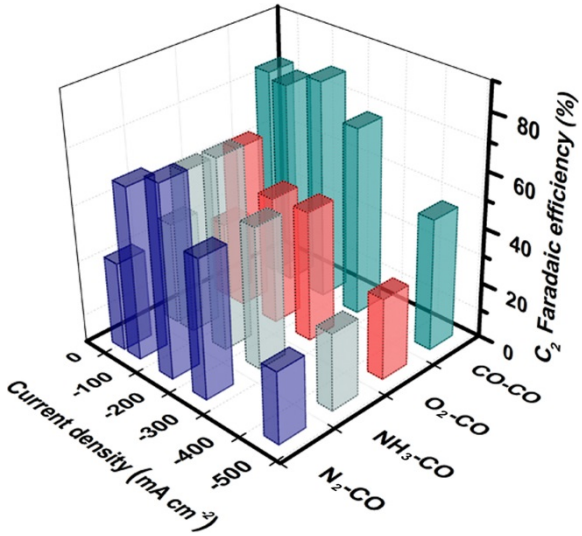

Fig. S18. C_2 FE of the N-Cu NPs/GDL at each given current density under different pre-reduction atmospheres. (For example, CO-CO means pre-reduction in a CO atmosphere and then a catalytic test in a CO atmosphere.)

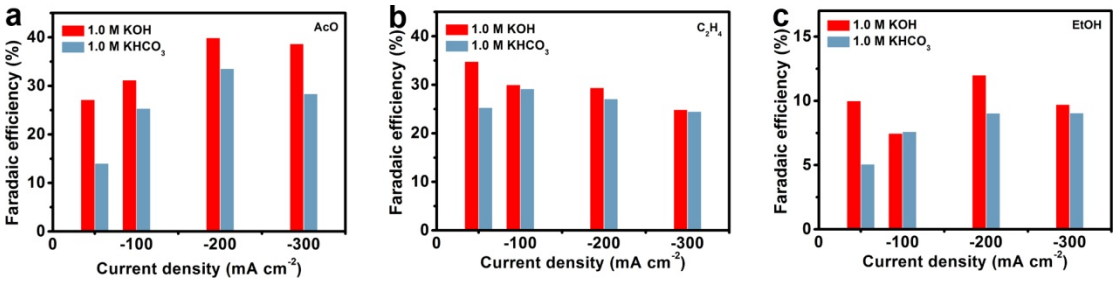

Fig. S19. (a) AcO, (b) C_2H_4 and (c) EtOH FEs of the N-Cu NPs/GDL at each given current density in different electrolytes.

Table S1. Comparison of the electrocatalytic CO reduction performance for Cu-based catalysts.

Catalyst	Electrolyte	C_{2+} FE (%) at -0.69 V vs. RHE	C_{2+} current density at -0.69 V vs. RHE (mA cm^{-2})	Maximum C_{2+} FE (%)	Potential (V vs. RHE, corresponding to the maximum C_{2+} FE)	C_{2+} current density (mA cm^{-2}, corresponding to the maximum C_{2+} FE)	Ref.
N-Cu NPs	1.0 M KOH	81.31	162.62	81.31	-0.69	162.62	This work
Polycrystalline Cu	0.1 M KOH	~58	~1.3	65	-0.63	~0.9	1
Fragmented Cu	1.0 M KOH	-	-	~80	-0.66	~100	2
Spherical Cu	0.1 M KOH	~62	~5	62	-0.78	100	3
Dendritic Cu electrodes	0.1 M KOH	~60	~14	~75	-0.83	~80	
Cu nanocavity	1.0 M KOH	~63	~40	68.7	-0.36	~10	4
Cu nanosheets	2.0 M KOH	~62	~62	70	-0.74	~155	5
Cu nanowires	0.1 M KOH	-	-	65	-0.30	0.22	6
OD-Cu	1.0 M KOH	~79	~800	80	-0.6	212.49	7
Cu–Ag	1.0 M KOH	-	-	79.2	-0.56	~26.4	8
$Ag_2Cu_2O_3$	1.0 M $CsHCO_3$	~79	~155	91.7	-0.86	550	9

PTFE-Cu particles	1.0 M KOH	~72.5	~16	72.5	-0.70	~16	10
Polycrystalline Cu foil	0.1 M KOH	~39	~0.9	~57	-0.6	~0.5	11
Cu nanoparticles	10 M KOH	~15.9	~38	17.8	-0.85	50.8	12
Cu nanowire	0.1 M $KHCO_3$	~12	-	60	-1.1	-	13
Cu single-atom/ $Ti_3C_2T_x$	1.0 M KOH	98 (-0.7 V)	~23	98	-0.7	22.1	14
Cu_3Ag	1.0 M KOH	~30	-	~60	-1.1	-	15
Small Cu nanocube	0.5 M $KHCO_3$	~5	<10	~40	-1.49	~44	16
Medium Cu nanocube		-	-	~60	-2.12	~240	
Large Cu nanocube		~6	<10	~65	-1.88	~117	
$Cu_{45.2}$/graphdiyne	1.0 M KOH	~87 (-0.7 V)	~156	91.2	-0.8	312	17

Refrence

1. L. Wang, S. A. Nitopi, E. Bertheussen, M. Orazov, C. G. Morales-Guio, X. Liu, D. C. Higgins, K. Chan, J. K. Nørskov, C. Hahn and T. F. Jaramillo, *ACS Catal.,* 2018, **8**, 7445–7454.
2. Y. Pang, J. Li, Z. Wang, C. Tan, P. Hsieh, T. Zhuang, Z. Liang, C. Zou, X. Wang, P. D. Luna, J. P. Edwards, Y. Xu, F. Li, C. Dinh, M. Zhong, Y. Lou, D. Wu, L. Chen, E. H. Sargent and D. Sinton, *Nat. Catal.,* 2019. **2**, 251–258.
3. J. Li, K. Chang, H. Zhang, M. He, W. A. Goddard, J. Chen and Q. Lu, *ACS Catal.,* 2019, **9**, 4709−4718.
4. T. Zhuang, Y. Pang, Z. Liang, Z. Wang, Y. Li, C. Tan, J. Li, C. T. Dinh, P. D. Luna, P. Hsieh, T. Burdyny, H. Li, M. Liu, Y. Wang, F. Li, A. Proppe, A. Johnston, D. H. Nam, Z. Wu, Y. Zheng, A. H. Ip, H. Tan, L. Chen, S. Yu, S. O. Kelley, D. Sinton and E. H. Sargent, *Nat. Catal.,* 2018, **1**, 946–951.
5. W. Luc, X. Fu, J. Shi, J. Lv, M. Jouny, B. H. Ko, Y. Xu, Q. Tu, X. Hu, J. Wu, Q. Yue, Y. Liu, F. Jiao and Y. Kang, *Nat. Catal.,* 2019, **2**, 423–430.
6. D. Raciti, L. Cao, K. J. Livi, P. F. Rottmann, X. Tang, C. Li, Z. Hicks, K. H. Bowen, K. J. Hemker, T. Mueller and C. Wang, A*CS Catal.,* 2017, **7**, 4467−4472.
7. M. Jouny, W. Luc and F. Jiao, *Nat. Catal.,* 2018, **1**, 748–755
8. X. Wang, Z. Wang, T. Zhuang, C. T. Dinh, J. Li, D. H. Nam, F. Li, C. Huang, C. Tan, Z. Chen, M. Chi, C. M. Gabardo, A. Seifitokaldani, P. Todorović, A. Proppe, Y. Pang, A. R. Kirmani, Y. Wang, A. H. Ip, L. J. Richter, B. Scheffel, A. Xu, S. Lo, S. O. Kelley, D. Sinton and E. H. Sargent, *Nat. Commun.,* 2019, **10**, 5186.
9. N. Martić, C. Reller, C. Macauley, M. Löffler, A. M. Reichert, T. Reichbauer, K. M. Vetter, B. Schmid, D. McLaughli, P. Leidinger, D. Reinisch, C. Vogl, K. J. J.

Mayrhofer, I. Katsounaros and G. Schmid, *Energy Environ. Sci.,* 2020, **13**, 2993–3006.

10. R. Chen, H. Su, D. Liu, R. Huang, X. Meng, X. Cui, Z. Tian, D. Zhang and D. Deng. *Angew. Chem.,* 2020, **132**, 160-166.
11. A. S. Malkani, J. Li, N. J. Oliveira1, M. He, X. Chang, B. Xu and Q. Lu, *Sci. Adv.,* 2020, **6**, 2569.
12. L. Han, W. Zhou and C. Xiang, *ACS Energy Lett.,* 2018, **3**, 855-860.
13. H. Zhang, Y. Zhang, Y. Li, S. Ahn, G. T. R. Palmore, J. Fu, A. A. Peterson and S. Sun, *Nanoscale*, 2019, **11**, 12075.
14. H. Bao, Y. Qiu, X. Peng, J. Wang, Y. Mi, S. Zhao, X. Liu, Y. Liu, R. Cao, L. Zhuo, J. Ren, J. Sun, J. Luo and X. Sun, *Nat. Commun.,* 2021, **12**, 238.
15. A. Guan, Q. Wang,aY. Ji, S. Li, C. Yang, L. Qian, L. Zhang, L. Wu and G. Zheng, *J. Mater. Chem. A,* 2021, **9**, 21779.
16. P. Zhu, C. Xia, C. Liu, K. Jiang, G. Gao, X. Zhang, Y. Xia, Y. Lei, H. N. Alshareef, T. P. Senftle and H. Wang, *Proc. Natl Acad. Sci.*, 2021, **118**, 2010868118.
17. W. Rong, H. Zou, W. Zang, S.o Xi, S. Wei, B. Long, J. Hu, Y. Ji and L. Duan, *Angew.Chem. Int. Ed.,* 2021, **60**, 466-472.